Elsevier Editorial System(tm) for Microelectronic Engineering
Manuscript Draft

Manuscript Number: MEE-D-12-00283R1

Title: A 2D MEMS grating based CMOS compatible poly-SiGe variable optical attenuator

Article Type: Research Paper

Keywords: Micro-opto-electro-mechanical systems (MOEMS), Variable optical attenuator (VOA), grating, monolithic integration

Corresponding Author: Mr. SUKUMAR RUDRA,

Corresponding Author's Institution:

First Author: SUKUMAR RUDRA

Order of Authors: SUKUMAR RUDRA; RITA VAN HOOF; JEROEN DE COSTER; GEORGE BRYCE; SIMONE SEVERI; ANN WITVROUW; DRIES VAN THOURHOUT

Abstract: A variable optical attenuator based on a 2D MEMS grating is described. The device is a perforated and suspended poly-SiGe membrane with fixed islands within the perforations. It specularly reflects light in the non-actuated state, whereas after actuation the membrane deflects downwards forming a grating which diffracts light in higher orders reducing the intensity of the specular reflection. Using a laser of 400 nm wavelength, we could obtain an attenuation level of 20 dB with 0.11 dB of polarization dependent loss. A close match was obtained between the experimental and simulated mechanical behavior of the device showing the possibility of efficiently extending its use in the NIR regime. Additionally, as the device is made of poly-SiGe deposited at low temperature, it can be monolithically integrated with CMOS in the future.

Cover Letter

Dear Editorial Board of Microelectronic Engineering,

Please find enclosed the manuscript named **"A 2D MEMS grating based CMOS compatible poly-SiGe variable optical attenuator"** by S. Rudra et al. All co-authors have seen and agreed with the contents of the manuscript. We certify that the submission is original work and is not under review at any other publication.

This work deals with novel 2D MEMS gratings made of Poly-SiGe, a novel material which can help in monolithically integrating MEMS directly on top of CMOS. It can appreciably reduce the cost and device dimension though the functionality increases manifold. We used the concept of 2D gratings in forming variable optical attenuators with applications mainly targeted towards optical communication. We showed a maximum attenuation level of ~20 dB at an applied voltage of 1.6 V. As the devices are based on symmetric 2D gratings, there is no polarization sensitivity for the diffracted light and hence we could obtain a maximum PDL of 0.11 dB at the highest attenuation level. We also tailored the design parameters to obtain a critical damped response for the devices showing a fast response time of 3.3 µs. Though the characterizations were performed with 400 nm laser, with proper simulations and explanations we support the efficient extension of its working range in the NIR regime. Supported by the SiGe technology, this can be a step forward in efficiently integrating large arrays of VOAs on a single silicon chip.

To our knowledge, this is the first 2D MEMS grating based VOA discussed thoroughly in literature. Hence, we hope that the editorial board and the reviewers will agree to the interest of this study.

Thanking you.

Yours sincerely,

Sukumar Rudra
Sint Pieternieuwstraat 41
Photonics Research Group
INTEC/ University of Gent
9000 Gent
Belgium
sukumar.rudra@intec.ugent.be

*Graphical Abstract (for review)

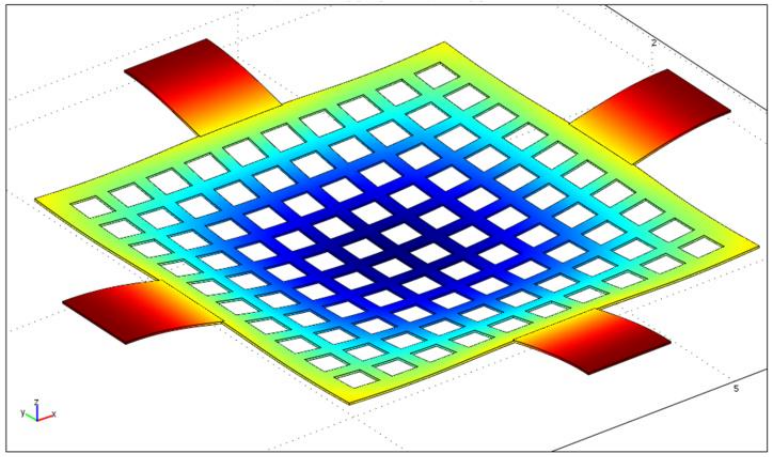

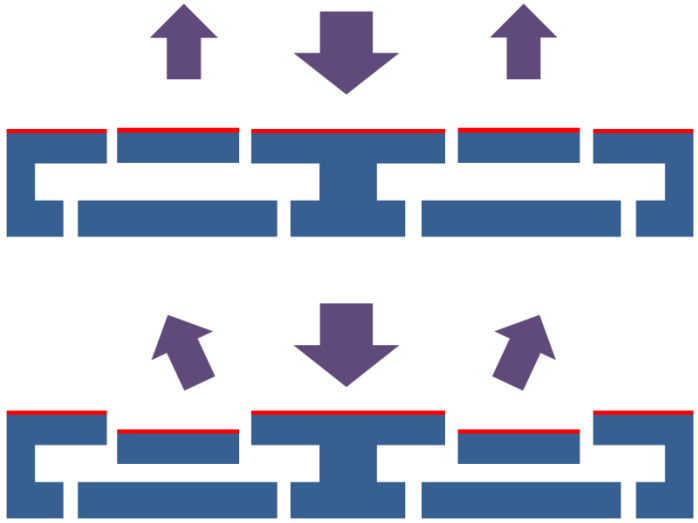

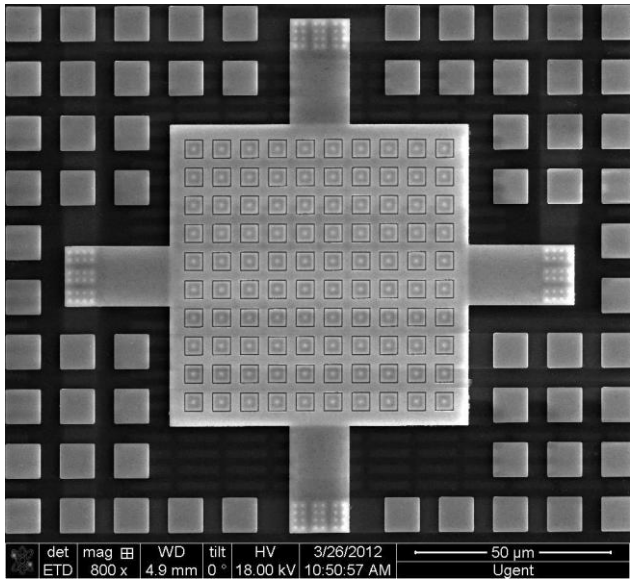

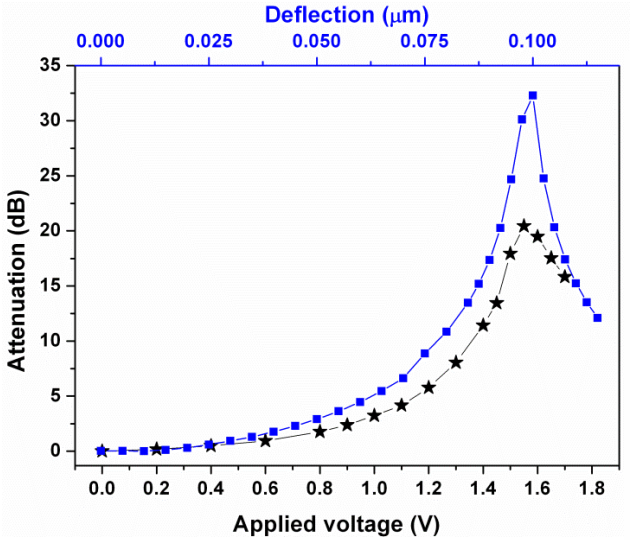

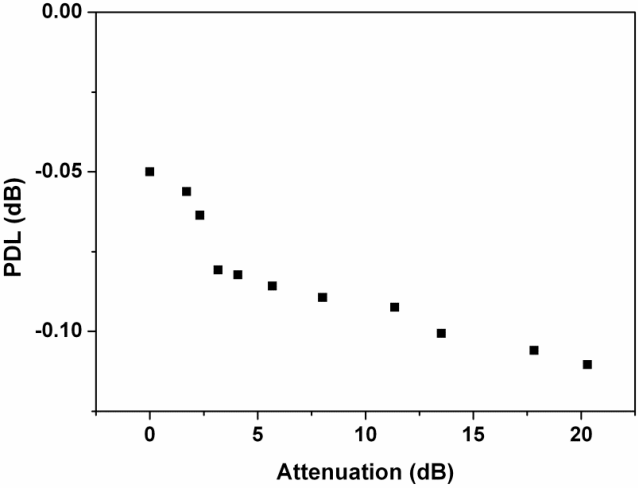

***Detailed Response to Reviewers**

Reviewers' comments:

Reviewer #1: A 2D MEMS grating based CMOS compatible poly-SiGe variable optical attenuator

S. Rudra, R. Van Hoof, J. De Coster, G. Bryce, S. Severi, A. Witvrouw, D. Van Thourhout

The authors report an alternative design for a Variable Optical Attenuator based on a MEMS structure. The device consists of a suspended poly-SiGe membrane with fixed islands within the holes of the photonic device. The reflectivity of the membrane can be tuned by electrostatic actuation of the membrane, which deflects downwards. This deflection forms a diffraction grating, reducing the specular reflection. Here are my comments:

- The paper is divided into different sections, after a brief introduction the authors introduce a conceptual depiction of the proposed structure, which is very useful. However, I missed a cartoon image in fig.1. Although it is in fig.2, it is not so clear. I strongly recommend merging fig.1 and fig.2 into only one. I also think that a 3D-like schematic depiction of the device could be very illustrative for a broad audience. This should be very easy by simply using the same files used for the fabrication tools.

-- Indeed merging Fig. 1 and Fig. 2 improves readability of the manuscript; hence we followed the reviewer's suggestion in the new revised version and joined both figures in the new Fig. 1. We did explore the possibility to provide a 3D-schematic but we believe the 2D cross-section better represents the diffractive operating mechanism of the device.

- Regarding the experimental characterization of the fabricated device, the actual experimental setup is not well described. I assume that the authors focus a laser spot on the membrane, collecting the reflection. However, I wonder how it is experimentally implemented. Are they shining the light perpendicularly to the membrane? In that case they have to use a beam splitter before the focusing objective. They say that the laser is linearly polarized, so I assume that they have a polarizing plate somewhere, as well as beam expander/collimator, and, of course, a photoreceiver. Maybe they are using an optical beam deflection technique. If this is the case, how it depends on the incident angle? What is the spot size on the membrane? I guess that the, since the curvature of the membrane in the actuated state is not zero, the actual measurements depend on the position of the spot on the surface. Please, consider a mayor revision of the experimental section.

--- In the revised version, the experimental set-up is now described in detail (Fig. 2). It is indeed a beam deflection technique that was used for the experimental characterization where we used perpendicular incidence of light on the membrane. The beam splitter helps in separating the incoming and outgoing light, whereas a photo detector measures the intensity of the diffracted orders. A quarter wave plate was used before the beam splitter to generate different polarization states and to find out the polarization dependent loss of the VOA.

Below we show the simulated version of the dependence of the attenuation on the incidence angle. As can be observed from the simulation, the maximum attenuation remains nearly the same though the deflection of the membrane at which it occurs changes with the angle of incidence. To our understanding, with higher incidence angle the vertical displacement (as seen

from that angle) of the membrane also needs to be higher (than the normal incidence) to reach the λ/4 level where the maximum attenuation occurs.

We were able to obtain a circular spot on the membrane with a diameter of 40 µm. The grating was mounted on a XYZ stage which was optimized accordingly and monitored with a microscope to ensure that the focused spot is incident right at the center of the membrane.

As mentioned above, we have changed the manuscript to make the description of the setup clearer.

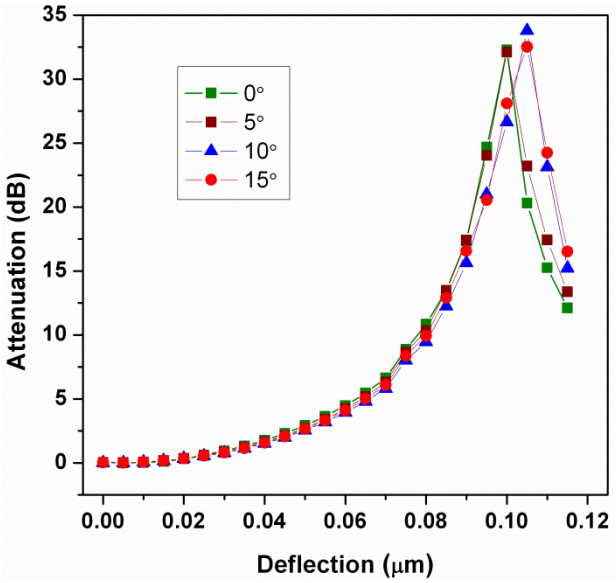

- The authors mention that they have used a Laser Doppler Vibrometer to characterize the mechanical behavior of the structure, but they do not show that measurement. I would like to see those measurements, or just an optical profile of the fabricated membrane.

If they have access to a spectrum analyzer and the bandwidth of the photodetector is large enough (350 kHz is not so high) it could be interesting to show a measurement of the mechanical resonance peak.

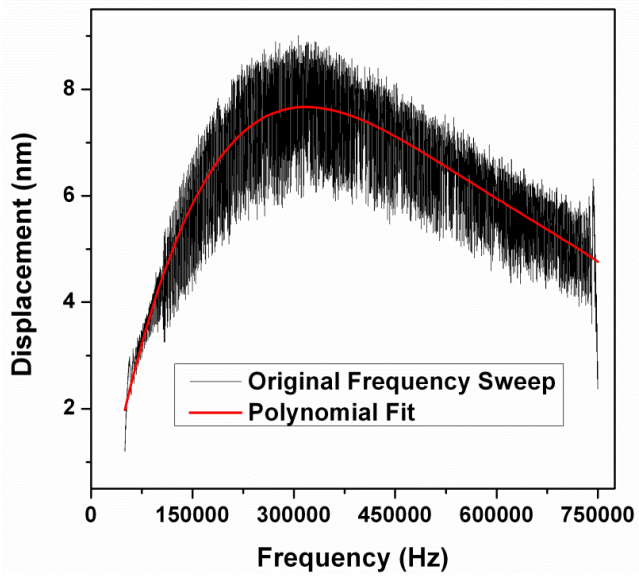

--- We used the Laser Doppler Vibrometer (LDV) to characterize the mechanical properties of the membrane. Particularly, the resonance frequency and the damping nature of the perforated membrane are of extreme importance as it determines the switching rate of the VOA.

Hence, we performed two different measurements using the LDV: (i) small signal frequency response to determine the resonance frequency and (ii) step response to determine the switching time.

The above figure shows the frequency sweep performed on the membrane which clearly shows a resonance peak at ~ 320 kHz. We did not include this particular measurement in the manuscript because we believe it adds little value beyond the resonance frequency already mentioned in the manuscript. We prefer to focus on the step response, which is described in detail in the manuscript (Fig. 6).

We did not use LDV to measure the optical profile of the membrane; however the manuscript does include (Fig. 4) a calculated profile of the membrane. Given the good agreement between simulation and experiments for other parameters we believe this simulation is representative for the actual profile.

- How can the authors control the initial bending of the membrane? Are they using any kind of stress relief in the supporting arms of the membranes? A lot of work has been done in this field. Please, say something about the measurements of the initial separation, fabrication errors, etc

--- No stress relief was applied in the supporting arms of the membrane. The deposition recipe was adjusted in such a manner that the structural poly-SiGe layer itself had an inherent tensile stress which helped in controlling (=avoiding) the initial bending of the membrane.

The mechanical properties (Young's modulus and tensile stress) of the structural poly-SiGe were measured by fitting the resonance frequencies of fixed-fixed beams of different lengths from which we found a Young's modulus of 120 GPa and a tensile stress of 20 MPa in the structural layer (S. Rudra *et al*, Static and dynamic characterization of pull-in protected CMOS compatible poly-SiGe grating light valves, Sensors and Actuators A, 179 (2012) 283-290). This is now also mentioned in the revised version.

- I couldn't find any word about the experimental measurement of the separation between the membrane and the substrate. Figs.3, 6 and 7 mention the separation as a parameter, how it was measured?

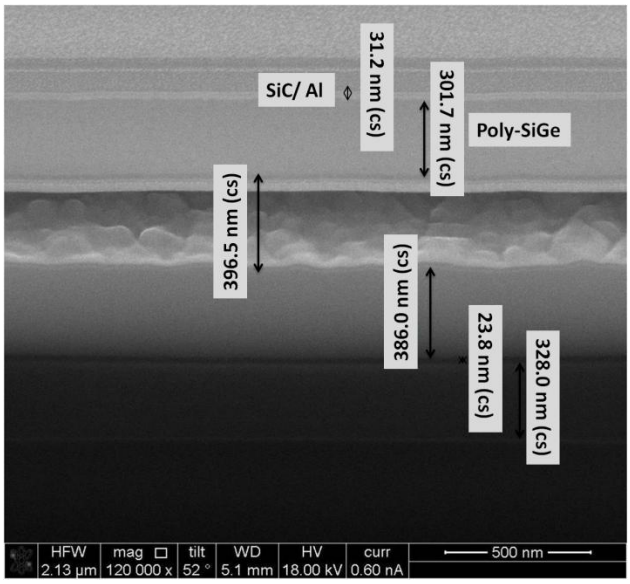

--- Initial measurement of the separation between the membrane and the substrate was performed by monitoring the thickness of the deposited sacrificial layer which was later confirmed by measuring the SEM cross section after releasing the structures. This is now clearly mentioned in the revised version of the paper.

Above, for the reviewer's interest, we also show the SEM cross-sectional measurement showing the thickness of the airgap (between membrane and substrate) and other layers. Given the little added value, we do not attach the picture in the manuscript.

As a general comment, I have to say that the potential interest of this paper is handicapped by the poor experimental section description. It could be easily solved by simply adding a schematic figure and a couple of paragraphs explaining the measurement setup.

--- As suggested by the reviewer, we did a major revision of the experimental section part.

I also think that a detailed (not so much, just simply few lines) explanation of the electrostatic actuation of the membrane is needed in this paper. Although it is not the scope of the presented work, a reader which is not familiar with this kind of actuation could be confused at some point. For example, the authors never mention the existence of an intrinsic limitation with the electrostatic actuation (1/3 the gap size). It is not necessary a detailed expression of the equations, but a couple of references would be appreciated.

--- Few extra lines are now added on the electrostatic actuation mechanism of the device and the related pull-in phenomenon. We also added a couple of extra references for the benefit of the readers.

Reviewer #2: The paper is well-written, describing experimental work, which is supported by simulations. The work is interesting and relevant for optical telecommunication and MOEMS communities. Background and motivation are clearly expressed and sufficiently cited in references. Figures are clear and illustrative. I have only few minor comments and proposals for corrections.

The paper contains many abreviations. Some of them are not written in brackets. For example:

- DFB-LD

- MARS modulator

- SiN (silicon nitride Si3N4 if stoichiometric in this case)

--- The first two abbreviations are now clarified in the revised text. For the 3rd one, as found from the original literature, it was not a stoichiometric Silicon Nitride and hence replaced with SiN_x in the revised text.

- B-doped (Obviously boron doped. Why membrane, being mechanical part of the device, needs to be boron doped ? What advantages does it provide ?)

--- The Boron doping has a two fold advantage: (i) it reduces the deposition temperature of the structural poly-SiGe layer and also (ii) the resistivity of the poly-SiGe layer is reduced which makes it of potential interest for low thermal budget application of MEMS that are post-processed on top of standard CMOS wafers with metallic interconnects. (S. Sedky *et al*, Effect of *in situ* boron doping on properties of silicon germanium films deposited by chemical vapor deposition at 400 °C, J. Mater. Res. 16 (2001) 2607-2611). This has now been mentioned in the text.

- CMP (Chemical Mechanical Polishing). CMP is used to adjust SiGe layer thickness to be 300nm. When talking about Lambda/4 and Lambda/2 layers, what is typical level of controlability and reporducibility of CMP ? +- 1nm or something else ? Is that trivial or state-of-art ?

--- Weight measurements were done after film deposition and CMP to calibrate the deposition thickness since optical measurements (ellipsometry) was not possible on the wafers. The reproducibility from one device to another device wasn't perfect. However this is not critical for our application: the Lambda/4 and Lambda/2 displacements forming the grating (and associated diffraction) are formed by actively controlling the membrane. So by optimizing the applied voltage small process changes can always be taken into account. The only important layer thickness is that of the sacrificial layer, which should be larger than $d>3\lambda/4$ (to avoid pull-in). But again, the exact thickness is not critical and is sufficient to take into account a safety margin which can accommodate process variability. Hence, though a state-of-the-art CMP is a privilege, a minor deviation doesn't influence the output quality.

- 320 KHz >> 320 kHz

--- This is also corrected in the revised text.

A 2D MEMS grating based CMOS compatible poly-SiGe variable optical attenuator

S. Rudra [a], R. Van Hoof [b], J. De Coster [b], G. Bryce [b], S. Severi [b], A. Witvrouw [b], D. Van Thourhout [a]

[a] Photonics Research Group, INTEC, Ghent University- IMEC, Gent, Belgium

[b] IMEC, Leuven, Belgium

Abstract:

A variable optical attenuator based on a 2D MEMS grating is described. The device is a perforated and suspended poly-SiGe membrane with fixed islands within the perforations. It specularly reflects light in the non-actuated state, whereas after actuation the membrane deflects downwards forming a grating which diffracts light in higher orders reducing the intensity of the specular reflection. Using a laser of 400 nm wavelength, we could obtain an attenuation level of 20 dB with 0.11 dB of polarization dependent loss. A close match was obtained between the experimental and simulated mechanical behavior of the device showing the possibility of efficiently extending its use in the NIR regime. Additionally, as the device is made of poly-SiGe deposited at low temperature, it can be monolithically integrated with CMOS in the future.

Keywords:

Micro-opto-electro-mechanical systems (MOEMS), Variable optical attenuator (VOA), grating, monolithic integration

Introduction:

Integrated variable optical attenuators (VOAs) have been widely used for actively controlling the optical power level in wavelength-division multiplexing (WDM) networks [1]. The widespread deployment of WDM networks demands VOAs with compact, robust designs with low power consumption and low wavelength dependent loss (WDL) [2]. Moreover, these VOAs should be able to dynamically regulate the WDM channel power irrespective of the incident light polarization. Additionally, in dense wavelength division multiplexing (DWDM) systems, it has become common to control the output of Distributed Feedback Laser Diodes (DFB-LD) with a VOA instead of the input current. Hence, with increasing number of wavelengths multiplexed in these networks, large arrays of VOAs preferably integrated on a single silicon chip will be needed for future DWDM applications. In addition, although the VOAs are now mostly used in telecommunication applications, there are other fields where VOAs are extremely useful. E.g. the membranes used in the absorbance based optodes which are susceptible to degradation due to excessive optical power [3]. Also, with increasing popularity of Visible Light communications (VLC), use of VOAs in the visible wavelength is becoming more and more popular [4].

Basically two different families of VOAs have been presented so far, namely those based on micro-optoelectromechanical systems (MOEMS) and those based on photonic lightwave circuits (PLC). Typically, MOEMS based VOAs offer physical features such as tunability, scalability, low electrical power consumption and small form factor [5]. Additionally, as the MEMS technologies use a semiconductor-like lithographic batch fabrication process, the micro-opto-mechanical components can be monolithically integrated (if the technologies used are thermally and material-wise compatible) with the control electronics on the same chip [6]. This not only improves the performance, yield and reliability but also lowers the manufacturing, packaging and instrumentation costs [7].

Out of the several different MOEMS based VOA designs proposed over the years, interference type VOAs are one of the most primitive and popular ones. The interference type VOA uses multi-beam interference to adjust the attenuation level. The first such design was the MARS (mechanical antireflection switch) modulator [8], in which a SiN_x membrane of λ/4 optical thickness was suspended over a silicon substrate with a fixed 3λ/4 spacing. When reflections from the top surfaces of the membrane and substrate are in phase, the incident light is totally reflected. But when the membrane is electrostatically lowered to an airgap of λ/2, it becomes an antireflection coating with strongly reduced reflectivity. Though the achieved attenuation level was 31 dB with < 3 μs of response time, the reported insertion loss was ~ 3 dB and the device had a relatively high actuation voltage of 35.2 V. An alternative design consists of a 1D deformable grating based VOA having two sets of grating lines where one is movable and the other is fixed on the substrate [9]. A contrast of 16 dB with a much lower driving voltage of 9.6 V was reported. But, as these gratings are actually a 1D array of very closely spaced suspended microbeams with subwavelength airgap and metallic coating, the specular reflection is a strong function of the state of polarization of the incident light [10].

In this paper we report an alternative design which can be used effectively in solving the polarization dependence of the grating based VOAs. We used poly-SiGe as the structural material as it has been demonstrated to be an ideal material for a MEMS-last monolithic process. Since, poly-SiGe films (deposition temperature ~ 450˚ C) with very good electrical and mechanical properties can be obtained at CMOS-compatible temperatures [11], it is highly suited for applications that need arrays of MEMS devices to be individually connected to the interfacing circuits [12]. Our device consists of a poly-SiGe based 2D MEMS grating built from an anchored membrane with symmetrically distributed square shaped perforations which are filled with fixed islands. Because of the planar symmetry of the design, any preferential reflectivity of the different polarization states is effectively eliminated. Also, because of the relatively large dimension of these membranes, the actuation voltage is sufficiently low, leading to minimal power consumption. The design was altered in such a manner that the moving membrane exhibits the optimal damping condition leading to a minimal switching time. Using a 400 nm laser, we obtained an attenuation of ~ 20 dB with a maximum polarization dependent loss of 0.11 dB and a switching time of ~ 3.3 μs. To our knowledge, this is the first functional CMOS compatible 2D MEMS grating to be reported.

Device concept:

The proposed structure is presented in Fig. 1a. It consists of a suspended (anchored on four different sides) square shaped membrane which is perforated symmetrically in both the in-plane orthogonal directions. Within these perforations, fixed blocks are created (Fig. 1b) which are supported by anchors of the same height as those supporting the membrane as shown in the cross sectional view in Fig. 1c. The design was made in such a manner that the area of the movable part and fixed parts are nearly the same. The membrane is held in tension so that it remains flat and forms a reflective surface in the non-actuated state (OFF state) giving specular reflection in the 0^{th} order. When actuated, the membrane is deflected vertically resulting into an entirely reconfigurable 2D diffractive element (ON state) producing increased diffraction in the higher orders (Fig. 1d). At a deflection of λ/4, the light reflected from the membrane and the top of the islands are exactly opposite in phase which results in total annihilation of the 0^{th} order intensity.

The electrostatic force on the membrane associated with the constant voltage drive mode is nonlinear and gives rise to the well known phenomenon of pull-in [13, 14]. The electrostatically actuated membrane collapses on the ground plane once the highest deflection exceeds approximately one-third of the airgap (d_0). Hence in the VOA structure, the airgap between the membrane and the underlying ground substrate is designed in such a manner that $d_0/3>\lambda/4$. The actuation voltage is therefore always maintained well

below the pull-in voltage, saving it from deterioration. The detailed background theory regarding the function of these movable gratings can be found elsewhere [15].

Device Fabrication:

The structural layer is a B-doped poly-SiGe layer with a thickness of 330 nm which was deposited by chemical vapor deposition (CVD) at a wafer temperature of 450° C on top of a Ti (5 nm) / TiN (10 nm) adhesion layer. The precursor gasses were SiH_4, GeH_4 and B_2H_6. The SiH_4: GeH_4 ratio equaled 0.9:1 and a B_2H_6 (1% in H_2) flow of 90 sccm was used at a wafer temperature of 450° C, resulting in an expected Ge concentration of 78%. Next, a CMP step was used on the SiGe structural layer for roughness reduction. This CMP step also reduces the thickness of the structural layer down to 300 nm. Then a barrier layer of 5 nm thick SiC and a 30 nm thick Al layer were further added on top of the structural poly-SiGe layer to increase the reflectivity of the structures. A 400 nm airgap was maintained between the membrane and the underlying electrode. Due to limits in the lithographic resolution, the separation between the moving and the stationary part of the structural layer was fixed at 300 nm. Thickness values of the different layers and the separation among them was later confirmed by SEM cross-sectional measurements of the functional devices. A detailed description regarding the step by step fabrication of the devices can be found in our earlier report [15].

By fitting the resonance frequency of fabricated fixed-fixed beams of different lengths to simulation results, a Young's modulus of 120 GPa and a tensile stress of 20 MPa were derived for the SiGe structural layer [15]. The inherent tensile stress within the poly-SiGe layer was helpful in avoiding the initial bending of the suspended membrane and to keep it flat.

Though we used devices of different dimensions, here we discuss the best results as obtained with a perforated membrane with a total dimension of 75 µm x 75 µm, forming a grating with period of 7.0 µm with a fill factor of 0.88. The device is suspended on its four sides by supports of 18 µm x 15 µm each, which are then attached to anchors at the outer parts (Fig. 1b).

Experimental results and discussions:

Optical characterizations:

The optical characterization of the proposed design was carried out using a linearly polarized laser of 400 nm wavelength. This wavelength was selected in accordance to the airgap (400 nm) between the substrate and the membrane in the designed device. Fig. 2 shows the experimental set-up used to characterize the VOA. The two convex lenses in the front act as a collimator. The lens in front of the grating focuses the light as a circular spot (~ 40 µm diameter) with uniform intensity on the center of the VOA membrane. The beamsplitter helps in separating the incoming and outgoing light. A photodiode in series with a filtering slit was used to measure the intensity of the 0^{th} diffracted order as a function of amplitude of the applied actuation voltage. Additionally, we used a quarter wave plate in front of the beamsplitter to generate the circularly or elliptically polarized light which was used in determining the polarization dependence of the VOA performance.

The device under investigation was mounted on a XYZ stage and was monitored with a microscope which helped us in finding the optimum position (center of the membrane) of the focused spot on the membrane giving rise to the maximum achievable attenuation. As we work with the 0^{th} diffraction order, a small change in the incidence angle does not significantly influence the efficiency and the attenuation of the gratings under investigation.

The insertion loss of the devices was found to be ~ 1.1 dB which is mostly associated with the fill-factor of the grating and the reflectivity of the top layer. We believe that, with finer lithographic precision, the fill factor can be increased further. Moreover, due to the higher reflectivity of Al in the NIR regime, the insertion loss will be even lower in that part of the spectrum. The attenuation as function of the applied voltage is shown in Fig. 3. A clear decrease in the 0^{th} order intensity (increasing attenuation) can be observed with increasing external DC bias. We could obtain a maximum attenuation level of ~ 20 dB with an operating voltage of 1.6 V. The experimental result was also compared to a theoretical calculation carried out using Rigorous Coupled Wave Analysis (RCWA) [16]. While the qualitative behavior matches well, the maximum attenuation level differs by approximately 10 dB between the experimental results and the RCWA based simulations. To understand this discrepancy, we also performed a COMSOL Multiphysics™ based simulation studying the deflection of the membrane when applying a voltage. Fig. 4 shows that the deflection is not uniform as assumed in the RCWA simulations, but that there is a maximum deflection right at the center of the membrane. Hence, light reflected from the off-center parts is less attenuated as compared to that reflected from the center of the membrane. More importantly, due to working with the 0^{th} order mode, the removal of stray light is more challenging in the experimental set-up and hence we experience a decreased contrast. The PDL was measured at different attenuation levels, as shown in Fig. 5. A maximum loss of 0.11 dB at the highest attenuation of 20 dB was obtained which supports our claim that this device operates as a polarization independent VOA.

One of the substantial advantages of MEMS based VOAs compared to bulk mechanical systems is their high response speed enabling faster data transfer. Hence, it was important to study the device dynamics of these MEMS gratings. Due to the small underlying airgap and fast operating speed, squeeze film damping [17] becomes the dominant damping mechanism affecting the dynamic response of the device. So, we used Laser Doppler Vibrometry (LDV) to characterize the mechanical behavior of the suspended membrane. A resonance frequency of 320 kHz was obtained for the device. We also studied the damping nature of the device through applying a square wave pulse train with 20 µs period. As evident from fig. 6, a critically damped response was obtained for the device with a settling time ~ 3.3 µs (equilibrium ± 2%). To cross-check the experimental result, the mechanical behavior of the membrane was studied further using COMSOL. These simulations match our experimental results well with a calculated resonance frequency of 343 kHz and a near critical damped response as shown in fig. 7. The close match between the experimental and simulated results shows that by properly optimizing the design parameters, fast settling time can be achieved even when the desired usable range is extended to the NIR regime.

We also calculated the expected wavelength dependent loss (WDL) for our devices in the C-band used for fiber based telecommunication using RCWA simulations. Fig. 8 shows the attenuation as function of the displacement of the membrane for different wavelength of the incident light. Over a 40 nm bandwidth and for an attenuation level of 15 dB there is a maximal variation of 0.9 dB.

Conclusion:

We showed the operation of a 2D grating based MEMS VOA fabricated using the robust poly-SiGe technology suitable for monolithically integrating the devices directly on top of CMOS. We obtained a maximum attenuation of 20 dB for the devices with a polarization dependent loss of 0.11 dB and a settling time of ~ 3.3 µs. We also showed a very close overlap between the experimental and theoretical results regarding the mechanical behavior of the membrane indicating the possibility of optimizing the settling time in case of an altered design geared towards the NIR regime. Overall, these results prove the usefulness of the poly-SiGe technology in fabricating high quality VOAs. Given the compatibility of this SiGe platform with post-CMOS processing, this can be a step forward in efficiently integrating large arrays of VOAs on a single silicon chip.

Acknowledgement:

We would like to thank the Flemish agency for Innovation through Science and Technology to support this work through the SBO GEMINI project.

References:

[1] H. Ishio, J. Minowa, K. Nosu, Review and status of wavelength-division-multiplexing technology and its application, Journal of Lightwave Technology, 2 (1984) pp. 448–463
[2] A. Liu, Photonics MEMS devices: Design, Fabrication and Control, CRC Press, 2009.
[3] M. Puyol, I. Salinas, I. Garcés, F. Villuendas, A. Llobera, C. Domínguez, and J. Alonso, "Improved integrated waveguide absorbance optodes for ion-selective sensing," Anal. Chem., 74 (2002), 3354–3361.
[4] A. M. Khalid, G. Cossu, R. Corsini, M. Presi, and E. Ciaramella, Hybrid Radio over Fiber and Visible Light (RoF-VLC) Communication System, in 37th European Conference and Exposition on Optical Communications, 2011, paper We.7.C.1.
[5] C. Lee and J. A. Yeh, Development and evolution of MOEMS technology in variable optical attenuators, J. Micro/Nanolith. MEMS MOEMS 7 (2008), 021003.
[6] R. Jablonski, M. Turkowski and R. Szewczyk, Recent Advances in Mechatronics, Springer, 2007.
[7] A. Witvrouw, CMOS-MEMS integration today and tomorrow, Scripta Materialia 59 (2008), 945–949.
[8] J. E. Ford and J. A. Walker, Dynamic spectral power equalization using Micro-Opto-Mechanics, IEEE Phot. Tech. Lett. 10 (1998) 1440-1443.
[9] O. Solgaard, F. S. A. Sandejas, and D. M. Bloom, Deformable grating optical modulator, Opt. Lett., 17 (1992) 688-690.
[10] E. Tamaki, Y. Hashimoto, O. Leung, Computer to plate printing using the Grating Light Valve device, in: Photonics West 2004, Micromachining and Microfabrication symposium, 2004, paper 5348-08.
[11] S. Sedky, A. Witvrouw, K. Baert, Poly-SiGe, a promising material for MEMS monolithic integration with the driving electronics, Sensors and Actuators A 97-98 (2002) 503-511.
[12] L. Haspeslagh, J. De Coster, O.V. Pedreira, I. De Wolf, B. Du Bois, A. Verbist, R. Van Hoof, M.Willegems, S. Locorotondo, G. Bryce, et al. Highly reliable CMOS-integrated 11MPixel SiGe-based micro-mirror arrays for high end industrial applications, in: Proceedings of IEEE International Electron Devices Meeting, 2008, pp. 1–4.
[13] G.M. Rebeiz, R.F. MEMS, Theory Design and Technology, John Wiley and Sons, 2003. pp. 21–31.
[14] D. Peroulis et al., IEEE Trans. Microwave Theory Techniques 51 (2003) 259–270.
[15] S. Rudra, J. De Coster, R. Van Hoof, G. Bryce, S. Severi, A. Witvrouw, D. Van Thourhout, Static and dynamic characterization of pull-in protected CMOS compatible poly-SiGe grating light valves, Sensors and Actuators A, 179 (2012) 283-290.
[16] M. G. Moharam and T. K. Gaylord, "Rigorous coupled-wave analysis of planar-grating diffraction," J. Opt. Soc. Am. 71 (1982), 811-818.
[17] M. Bao and H. Yang, Squeeze film air damping in MEMS, Sensors and Actuators A, 136 (2007) 3–27.

Figure captions:

Fig. 1: SEM pictures of the top view of the full device with the attaching supports (a), zoomed-in view of the perforated membrane filled with the fixed islands (b), cross sectional schematic and working principle of the device in the non actuated state (c) and in the actuated state (d).

Fig. 2: Schematic of the optical set-up used to characterize the attenuation of the device.

Fig. 3: Comparison of the experimental and theoretical attenuation of the proposed device.

Fig. 4: COMSOL modeling of the electrostatic displacement of the membrane.

Fig. 5: Change in PDL with attenuation of the device.

Fig. 6: Step-response to a square wave pulse train showing a critical damped nature of the device.

Fig. 7: Simulated step response of the device showing a near critical damped behavior.

Fig. 8: Wavelength dependent attenuation characteristics of the device as simulated using RCWA.

Highlights:

- Novel CMOS compatible poly-SiGe variable optical attenuator with possibility of monolithically integrating the devices directly on top of CMOS.
- Very low polarization dependent loss of 0.11 dB at an attenuation of 20 dB.
- Fast switching speed (~ 3.3 μs).
- The first 2D MEMS based grating to be discussed in literature to our knowledge.

Figur

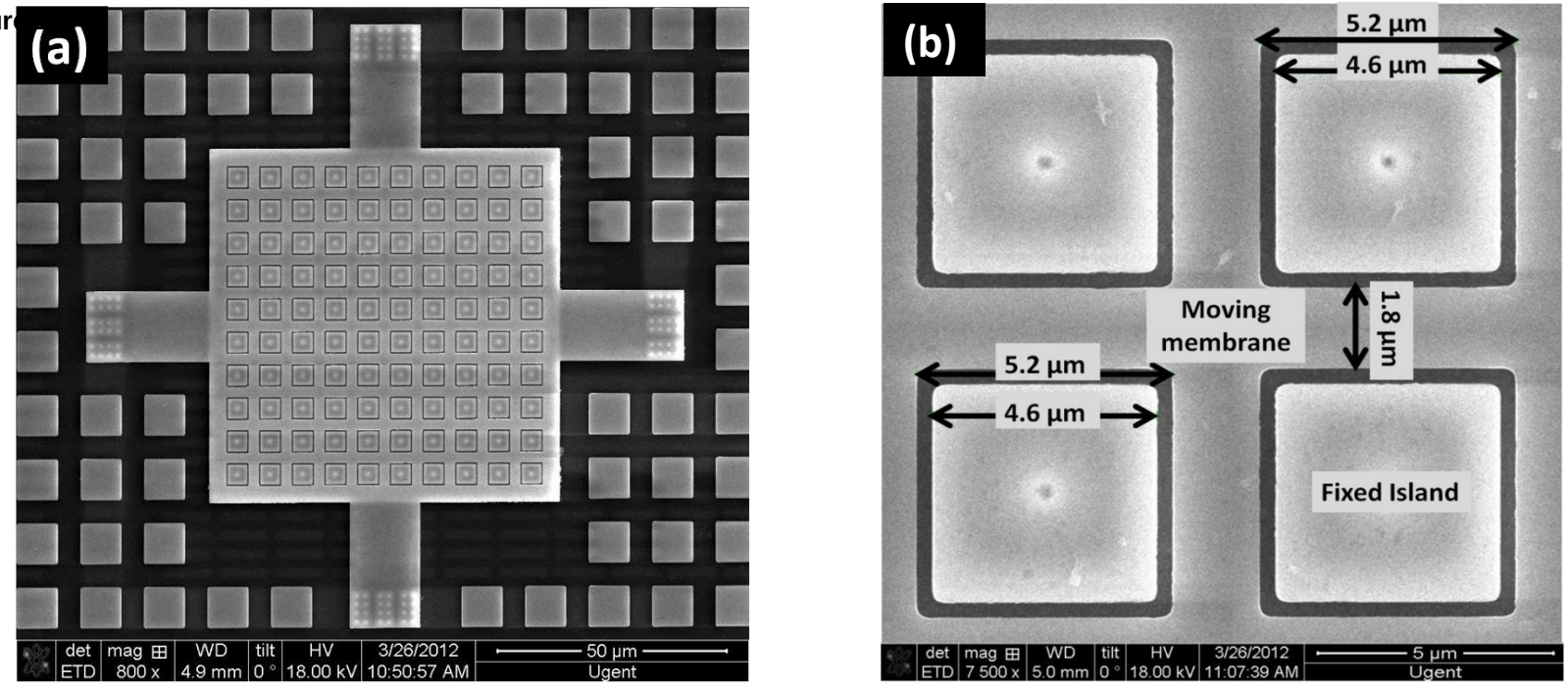
(a)
det ETD
mag 800 x
WD 4.9 mm
tilt 0 °
HV 18.00 kV
3/26/2012 10:50:57 AM
50 µm
Ugent
(b)
5.2 µm
4.6 µm
Moving membrane
1.8 µm
5.2 µm
4.6 µm
Fixed Island
det ETD
mag 7 500 x
WD 5.0 mm
tilt 0 °
HV 18.00 kV
3/26/2012 11:07:39 AM
5 µm
Ugent

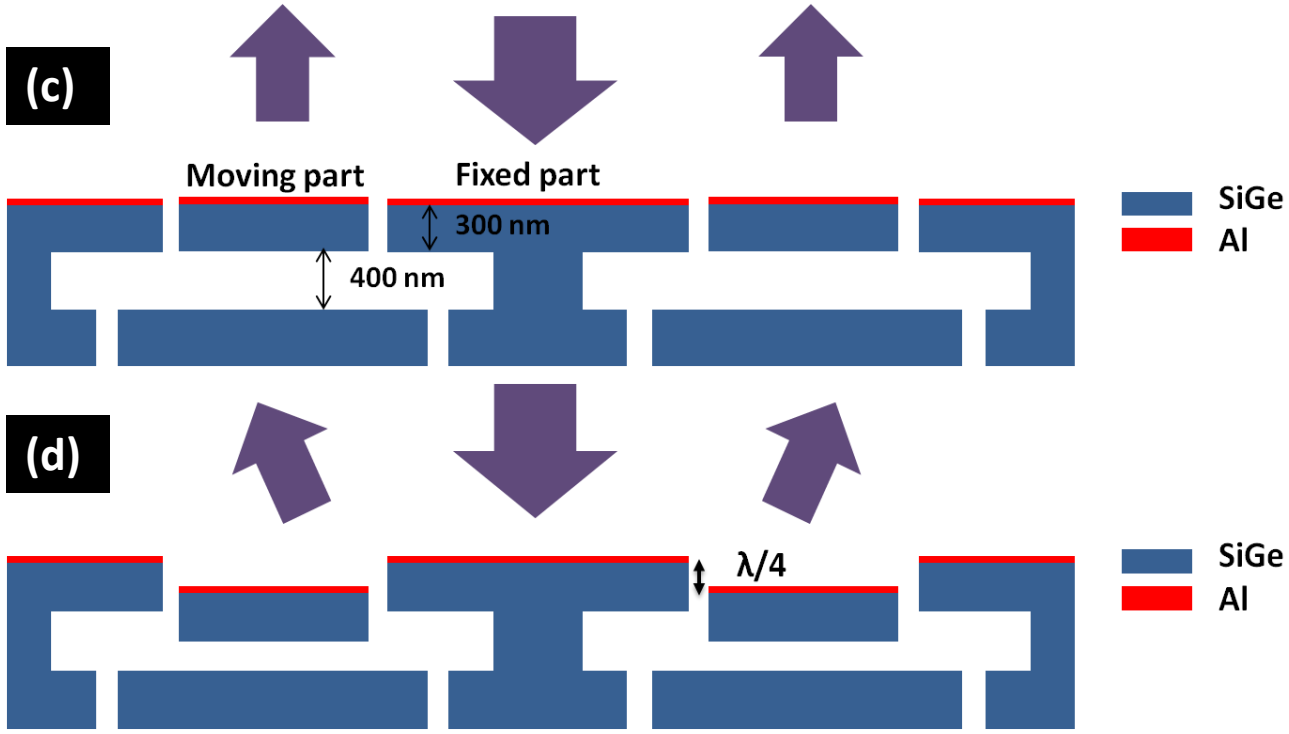
(c)
Moving part
Fixed part
300 nm
400 nm
SiGe
Al
(d)
λ/4
SiGe
Al

Figure 2

Click here to download high resolution image

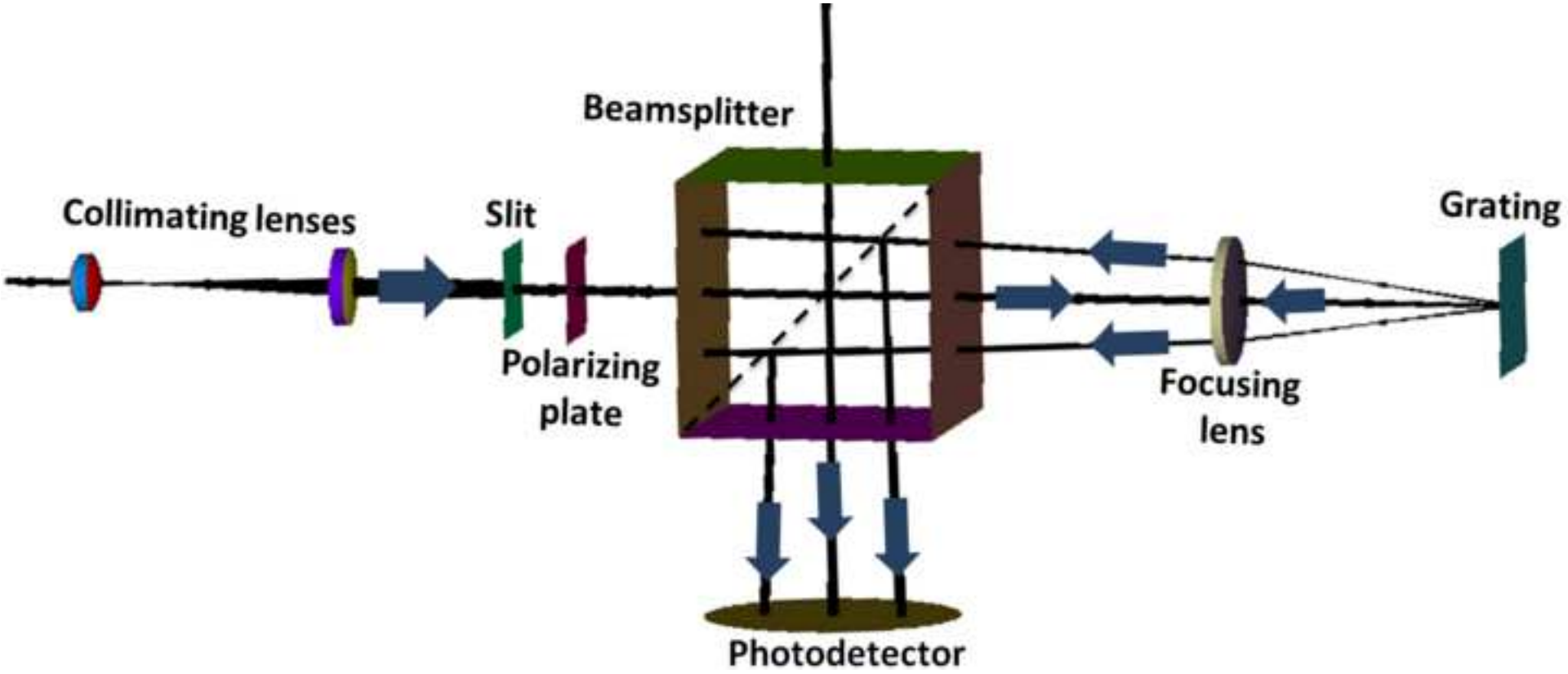

Figure 3

Click here to download high resolution image

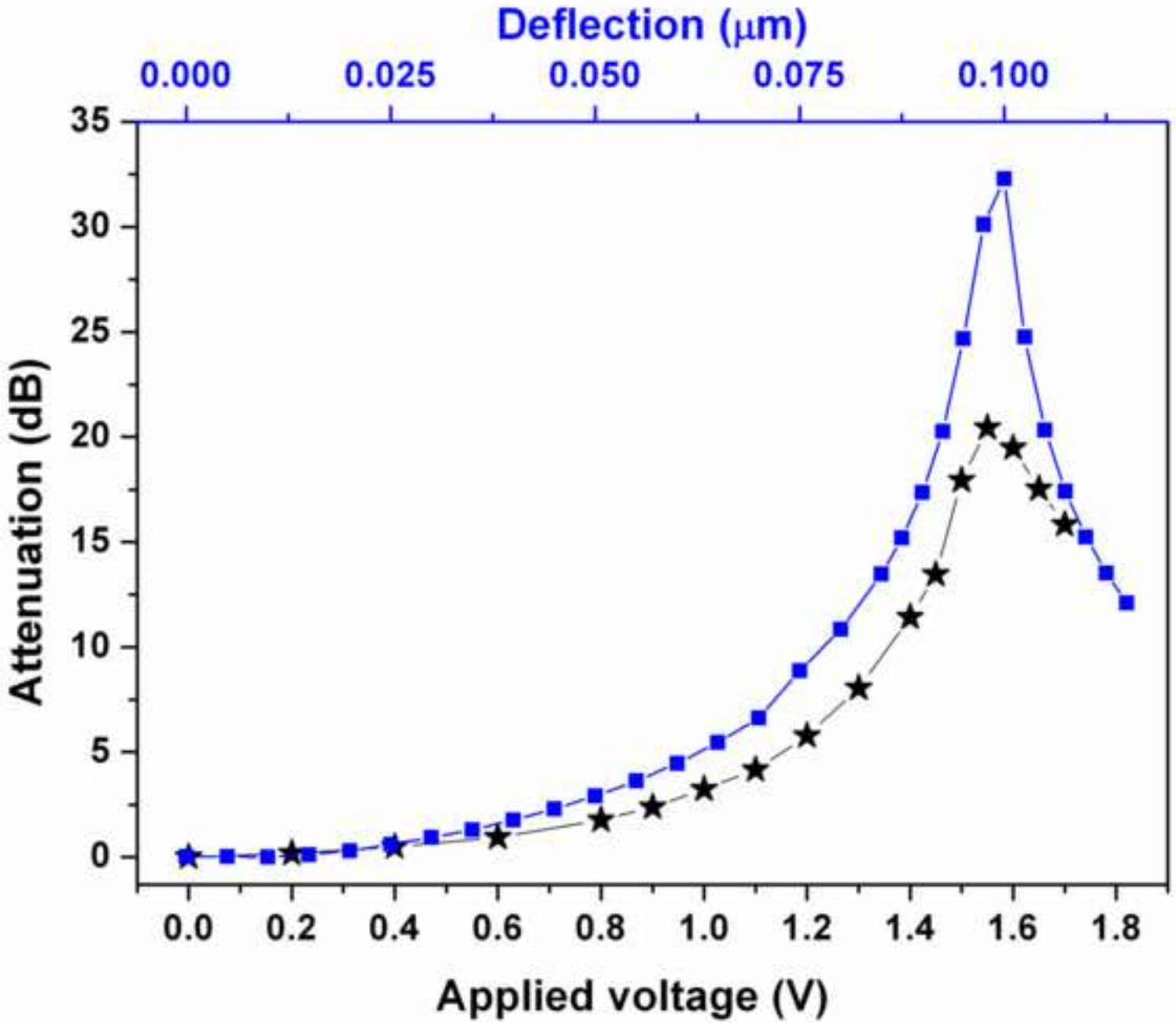

Figure 4

Click here to download high resolution image

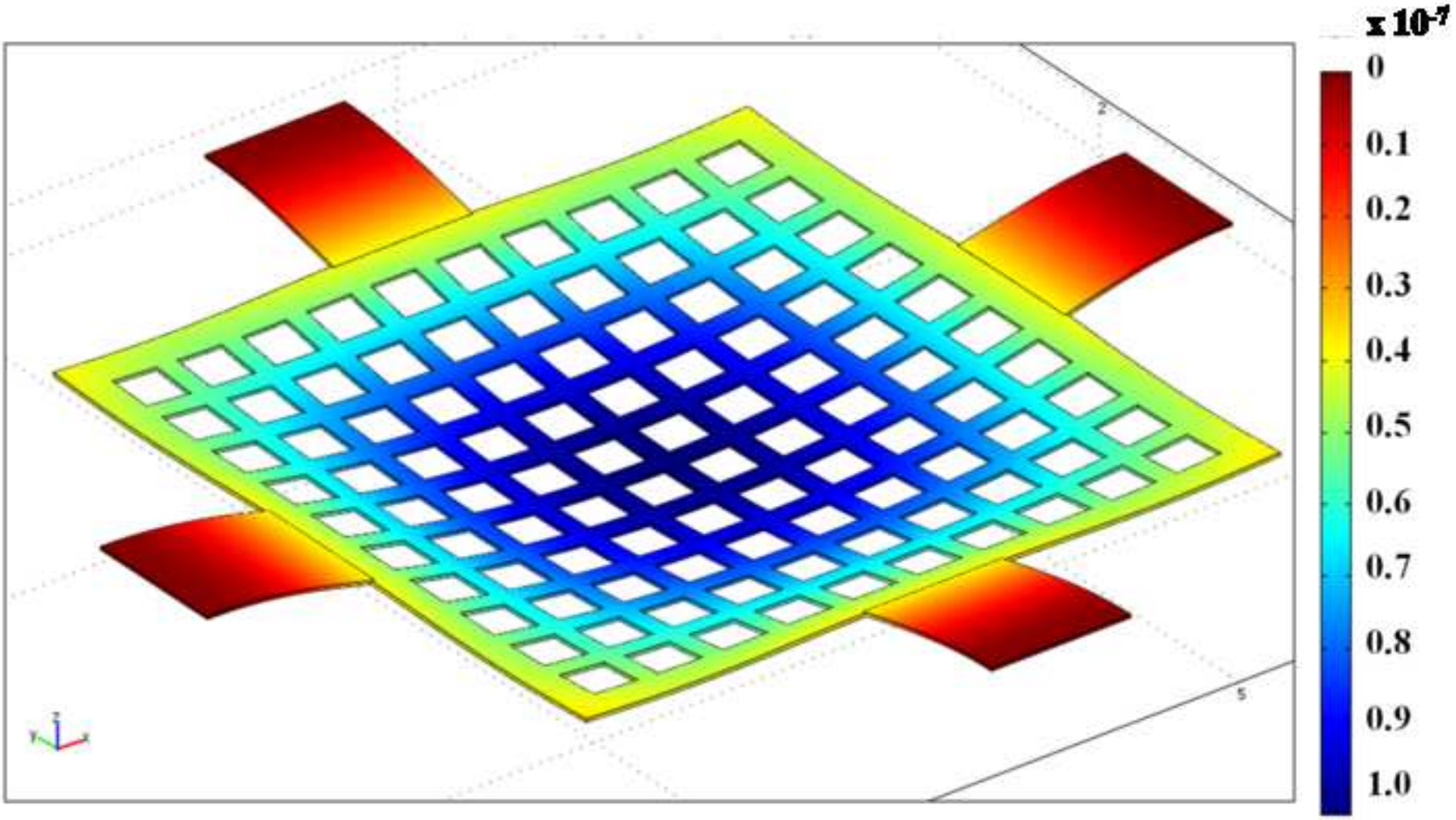

Figure 5
Click here to download high resolution image

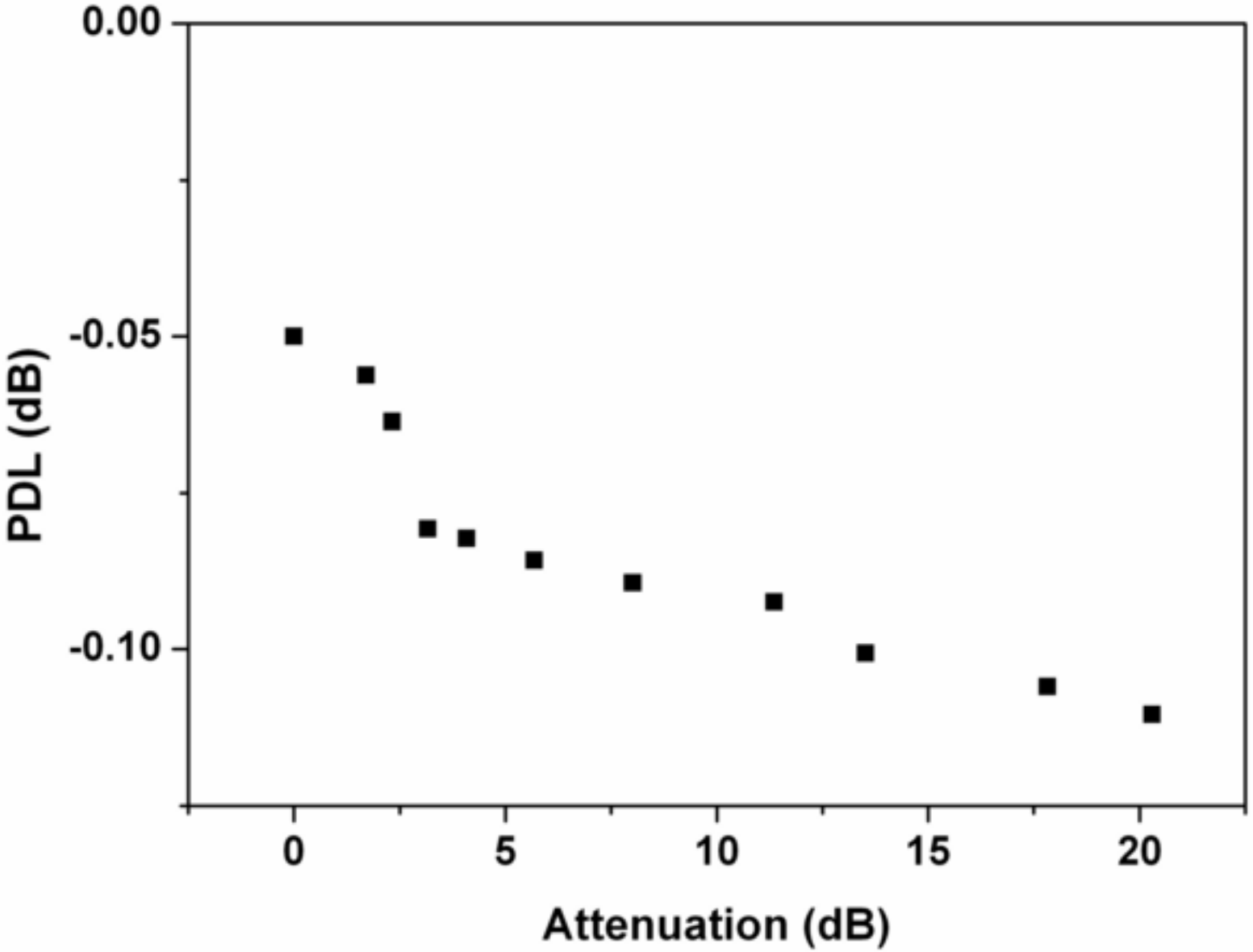

Figure 6
Click here to download high resolution image

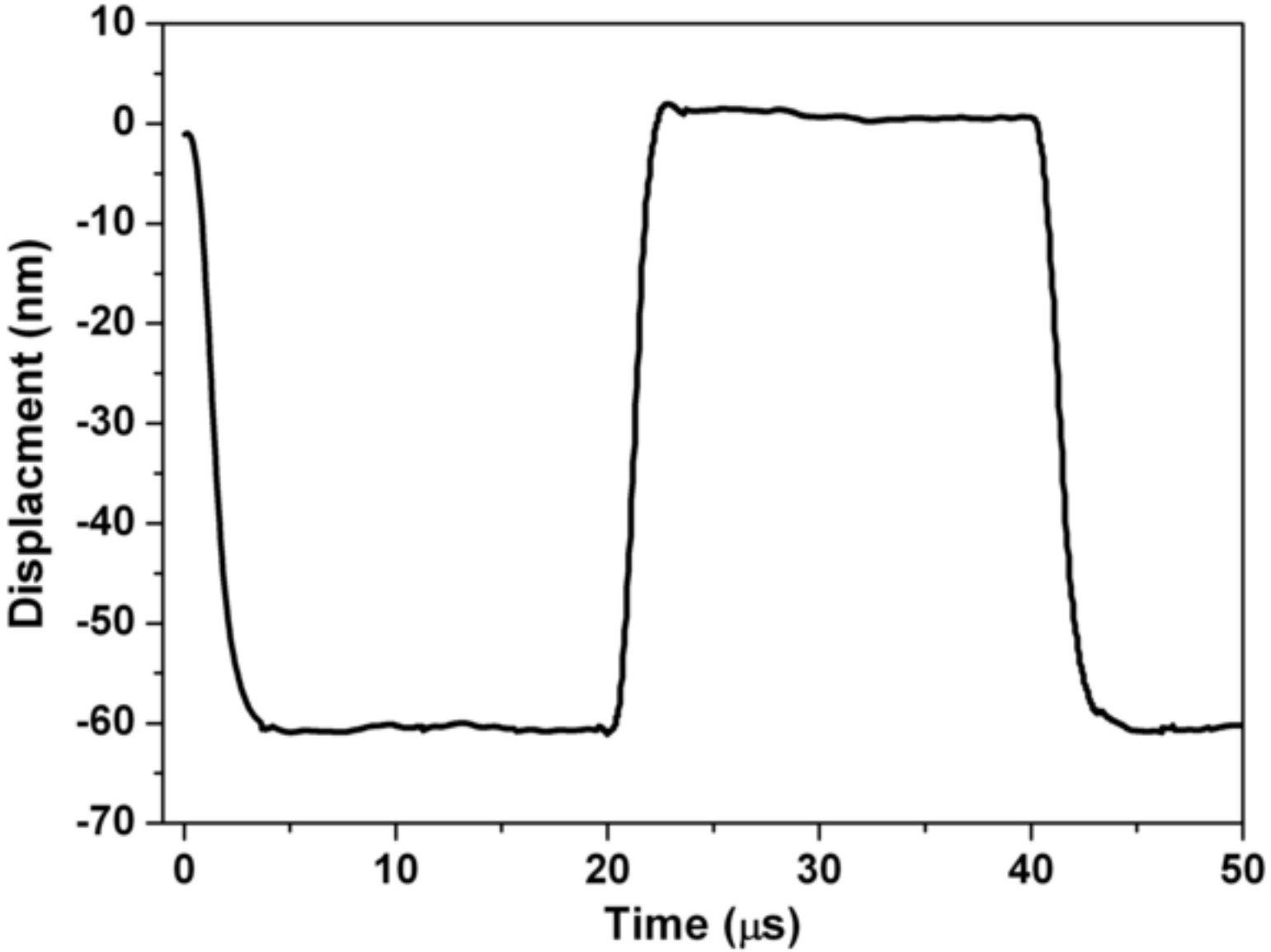

Figure 7
Click here to download high resolution image

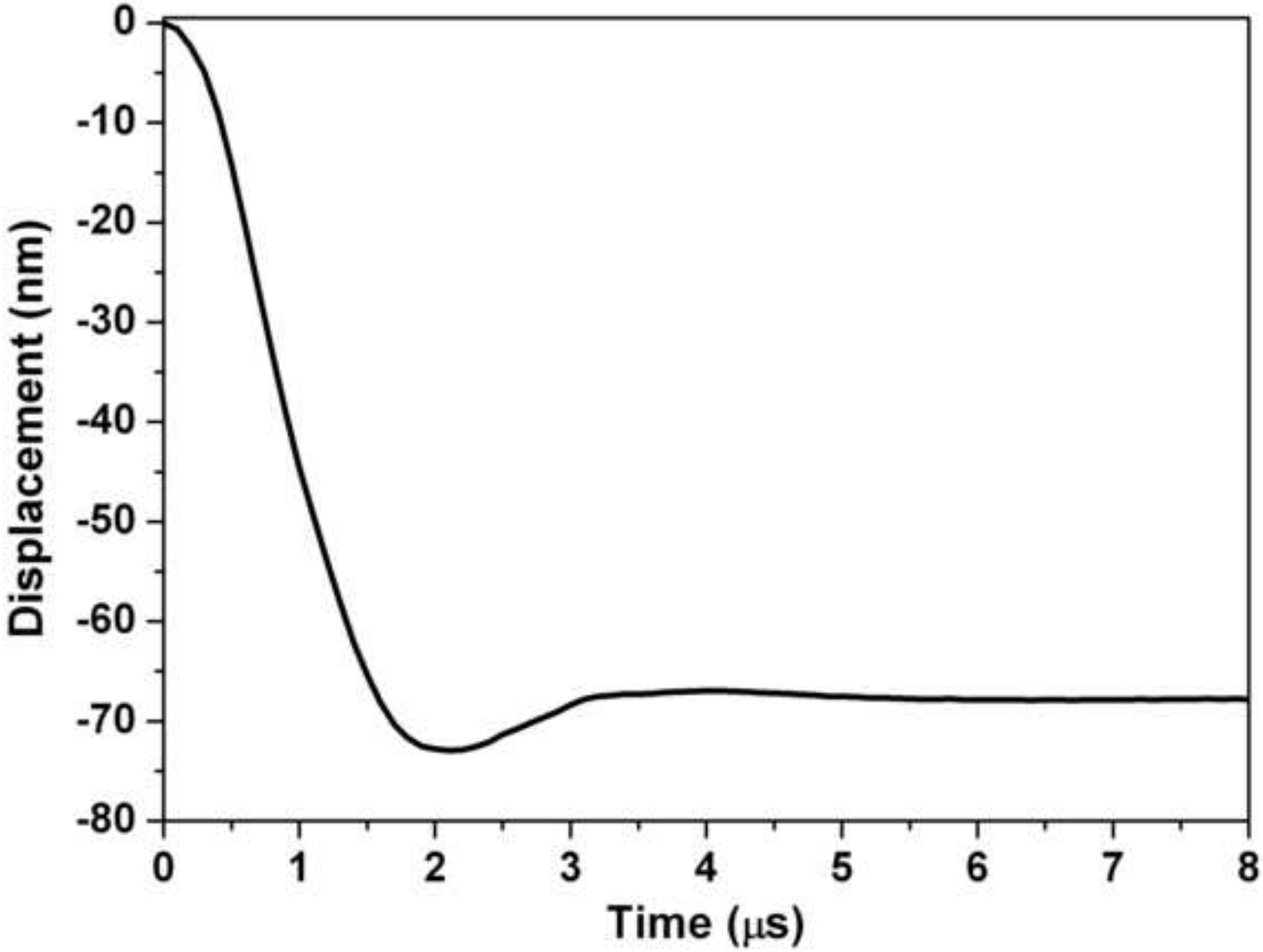

Figure 8

Click here to download high resolution image